Acquisition duration in resting-state arterial spin labeling. How long is enough?

Corentin Vallée, Pierre Maurel, Isabelle Corouge, Christian Barillot

▶ **To cite this version:**

Corentin Vallée, Pierre Maurel, Isabelle Corouge, Christian Barillot. Acquisition duration in resting-state arterial spin labeling. How long is enough?. Frontiers in Neuroscience, 2020, 14, 10.3389/fnins.2020.00598 . inserm-02129799v2

HAL Id: inserm-02129799

https://inserm.hal.science/inserm-02129799v2

Submitted on 18 Sep 2019

HAL is a multi-disciplinary open access archive for the deposit and dissemination of scientific research documents, whether they are published or not. The documents may come from teaching and research institutions in France or abroad, or from public or private research centers.

L'archive ouverte pluridisciplinaire **HAL**, est destinée au dépôt et à la diffusion de documents scientifiques de niveau recherche, publiés ou non, émanant des établissements d'enseignement et de recherche français ou étrangers, des laboratoires publics ou privés.

frontiers

Acquisition duration in resting-state arterial spin labeling. How long is enough?

Corentin Vallée [1,*], **Pierre Maurel** [1], **Isabelle Corouge** [1], **Chrisitan Barillot** [1]

[1] *Univ. Rennes, Inria, CNRS, IRISA, Inserm, Empenn U1228, Campus de Beaulieu, F-35042 Rennes*

Correspondence*:
Corentin Vallée
corentin.vallee@irisa.fr

ABSTRACT

Resting-state Arterial Spin Labeling (rs-ASL) is a rather confidential method compared to resting-state BOLD but drives great prospects with respect to potential clinical applications. By enabling the study of CBF maps, rs-ASL can lead to significant clinical subject-scaled applications as CBF is a biomarker in neuropathology. An important parameter to consider in functional imaging is the acquisition duration. Despite directly impacting practicability and functional networks representation, there is no standard for rs-ASL. Our work here focuses on strengthening the confidence in ASL as a rs-fMRI method and on studying the influence of the acquisition duration. To this end, we acquired a long rs-ASL sequence and assessed the quality of typical functional brain networks quality over time compared to gold-standard networks. Our results show that after 14 min of duration acquisition, functional networks representation can be considered as stable.

Keywords: Functional Magnetic Resonance Imaging, Arterial Spin Labeling, Resting-state fMRI, Acquisition duration, Modeling

1 INTRODUCTION

Functional MR imaging (fMRI) builds the links between location and function in the brain. The two main sub-domains in fMRI are task-based fMRI and resting-state fMRI. In task-based fMRI, a functional location is considered to be where the acquired signal matches with the task guidelines given to the subject. In resting-state fMRI, as no task is given, the focus is on fluctuations in voxels time-series induced by spontaneous neural activations. Similarities in these time-series in different areas have shown to be not random, but matching function of the brain (1). These similarities define the *functional connectivity* of the brain and show the underlying cerebral architecture organized into functional specialized units communicating with each other. Resting-state functional imaging aims to identify functional areas of the brain and depict how they interact outside any structural connectivity consideration (2) . Healthy and diseased subjects differ in functional networks cartography and in the intensity of functional connectivity for major disorders such as Parkinson's disease (3), Alzheimer's disease (4), severe depression (5) or schizophrenia (6).

Another subdivision in fMRI concerns the way the signal is obtained. The two major techniques are Blood Oxygen Level Dependent (BOLD) fMRI and functional Arterial Spin Labeling (fASL). Based on neurovascular coupling effects, BOLD techniques rely on the local signal variation induced by the neuron consumption of blood oxygen. Arterial Spin Labeling (ASL) is an MRI perfusion technique which uses magnetically labeled arterial water protons as an endogenous tracer. An inversion pulse labels the inflowing blood and after a delay called post-labeling delay, a labeled image of the volume of interest is acquired. The

subtraction of the labeled image from a control image, i.e., non labeled, reflects the quantity of spins that have perfused the imaged volume, producing what is commonly called a perfusion-weighted (PW) image.

The PW map can be used to quantify the cerebral blood flow (CBF) under some assumptions (7, 8). The quantification of CBF is the main advantage of ASL over BOLD. Indeed, the latter provides an indirect and non-quantitative measurement of neural activity, as it results from a combination of variations in CBF, cerebral blood volume and cerebral metabolic rate of oxygen. While the pathologies mentioned above were studied with BOLD, ASL allows to study a new set of pathologies with fMRI, such as acute stroke (9) or chronic fatigue syndrome (10) since CBF abnormalities can characterize pathologies.

The main drawback of ASL is its lower signal-to-noise ratio compared to BOLD fMRI. The repetition time (TR) is also twice to three times higher in fASL compared to BOLD fMRI, which impacts its temporal resolution. Furthermore, ASL can be implemented through numerous MRI sequences and meta-analyses can be difficult to set up, for ASL shows a high sequence parameter dependency (11, 12). Nevertheless consensus seems to overcome with years (13). Predominant in clinical usage and in academic research, BOLD is still considered as the gold standard in fMRI. However, as it provides quantification of CBF, ASL can be a serious contender to BOLD when it comes to pathologies evaluation, especially for Alzheimer's disease (14, 15, 16). The absence of contrast agent injection makes ASL well suited for longitudinal studies, particularly for pediatric population or for population with poor venous access or contrast agent contraindication.

The acquisition duration is an important parameter in an rs-fMRI study with strong practical consequences. Most current studies work with a duration from 8 min to 13 min and a TR from 3 s to 4 s (i.e. 120 to 260 images). Intuitively, one would assume the longer the duration, the better the sampling of the signal correlation across the brain and thus the better the acquisition. But this requires to define what "better" actually means and does not consider the practical questions of clinical implementation and subject resting-state upholding. To the best of our knowledge, some papers already studied the influence of duration in rs-BOLD (17, 18, 19, 20, 21), whereas in rs-ASL, it has not been explored yet. In this work, we first focus on the feasibility of detecting functional connected regions of the brain from rs-ASL. We remain as close as what a typical investigator of rs-ASL would experience by implementing usual sequence, processing and functional networks detection methods. We then assess a trend over the duration influence on rs-ASL detected networks quality: we do not directly assess whether an acquisition is good at a given time, but rather how it evolves with longer durations. After describing the scores used and the modeling approach, an in-depth analysis for the Default-Mode Network (DMN) will be presented in order to illustrate scores evolution on the most typical resting-state network. Finally, we will show results for all the functional networks under consideration and discuss an optimal sequence duration in rs-ASL.

2 MATERIAL

2.1 Subjects

Seven healthy male right-handed subjects aged from 21 to 28 years (23.5 yo$\pm$2.5) were involved in this study. All subjects gave informed written consent before participating in the study. We have maintained the homogeneity of the population in order to limit the influence of factors such as gender or age.

2.2 MR Acquisitions

The subjects were scanned on a 3.0T whole body Siemens MR scanner (Magnetom Verio, Siemens Healthcare, Erlangen, Germany) with a 32-channel head coil. A 3D anatomical T1-weighted MP2RAGE

image was acquired for each subject. The resting-state ASL imaging was performed using a 2D EPI pseudo-continuous (pCASL) sequence. Subjects were asked to keep their eyes closed, to relax (mind-wandering) without falling asleep. We used the most common parameters reported in the literature: TR = 3500 ms, FoV = 224 x 224 mm^2, TE = 12 ms, LD = 1500 ms and a 1250 ms post-labeling delay (PLD). Volumes were made of 24 slices of 64×64 voxels with 5 mm slice thickness with 20% gap for a total resolution of $3.5 \times 3.5 \times 6\,mm^3$. The number of volumes was 420 for a total duration of 24 min 30 s. For the 1250 ms PLD, we chose a balance between a longer duration, about 1800 ms, recommended to optimize the quality of the CBF estimate (13, 22), and a shorter duration, 600 ms, which seems to give a better functional representation (23, 24). We kept the PLD quite long as the main advantage of ASL is ultimately to compute CBF although we will focus on functional areas representation in this paper.

2.3 Data preprocessing

For each subject, the raw pCASL series is divided into 46 sub-series. The duration of these sub-series ranges from nearly 2 min (34 volumes) to 24 min 30,s (420 volumes) with a time step of 30 s. For the sake of simplicity, we will only mention rounded durations hereafter. All these subdivisions are made *before* any preprocessing: the preprocessing is done independently on each sub-series. For the preprocessing steps and their parameters we chose the most common ones found in bibliography. All steps are shown in Figure 1. For the preprocessing steps we used Matlab CONN toolbox (www.nitrc.org/projects/conn, RRID:SCR_009550) (25).

3 METHODS

3.1 Detecting networks with Seed-Based Analysis

To obtain the mapping of invidivual functional networks, we rely on seed-based analysis (SBA) (2). The principle of this method, the first proposed to define functional connectivity (1), is quite straightforward. Considering a similarity measure (usually linear correlation, but many others exist (26)), SBA builds functional areas by gathering voxels which exhibit a matching signal, in the sense of the chosen measure, to that of a ROI, called the seed in this context. Even if SBA is a very polymorphic modeling method, we use its most common form in our work. Hence we consider linear correlation as the similarity measure and use a set of 20 single voxels as seeds. Seeds are spread in the expected location of six usual functional networks: DMN, Sensori-motor, Language, Salience, Visual and Cerebellum. The exact positions of the seeds in the MNI152 space are provided in the appendix section and were suggested by the CONN toolbox. To build a functional map for each seed, we statistically test whether the signal between the seed and a candidate voxel is positively correlated with a risk of 1% FWER-corrected. This is a tough conservative testing compared to most of rs-ASL (even fMRI in general) studies, but we agree with the recommendation of (27) on false positive underestimation in fMRI litterature.

3.2 Evaluation scores

The resting-state BOLD litterature suggests different acquisition durations: 6 min (17), 10 min (18), 12 min (19), 25 min (20), and even 100 min (21). The main reason of their apparent discrepancy is the modeling. Indeed, there is many ways to properly define a model to assess to role of acquisition duration (a fortiori how much duration is enough), even if they lead to different conclusions. As a pioneer work on rs-ASL, we want our modeling to reflect an investigator experience with the impact of acquisition duration on functional network estimation. Figure 2 illustrates the investigation of acquisition duration we will model. The DMN estimation is validated after 14 min on Figure 2 because it matches with how

the functional network is expected to look like. In modeling terms, it is basically assessing the overlap of the estimated network with a reference network. In order to investigate a trend afterwards and decide which acquisition duration is enough, the individual functional maps will be compared to a reference, like process described in Figure 2. For that purpose, we rely on the Multi-Subjects Dictionary Learning atlas (MSDL) by (28). MSDL is an atlas of 17 resting-state functional networks containing our 6 networks of interest, and from which our seeds are independent. The key idea is to have functional maps close to what an expert would expect to observe when looking for the typical functional areas investigated here. To study the quality of the detected networks as a function of the acquisition duration, we evaluate the overlap between the SBA estimated functional maps and the MSDL references (simply called "reference" hereafter) through two measures: the Jaccard's index and the area under curve (AUC).

Let $\mathbb{E}$ be a set, let $(v_i)_{i\leqslant k\in\mathbb{N}}$ be observations in $\mathbb{E}$ and $(M_1; M_2) \in \{0; 1\}^{\mathbb{E}} \times \{0; 1\}^{\mathbb{E}}$ binary categorical variables. Let A,B,C,D be four sets with respective cardinals a,b,c,d defined by:

$$\begin{cases} A \coloneqq \{v_i \mid M_1(v_i) = 1, M_2(v_i) = 1\} \\ B \coloneqq \{v_i \mid M_1(v_i) = 1, M_2(v_i) = 0\} \\ C \coloneqq \{v_i \mid M_1(v_i) = 0, M_2(v_i) = 1\} \\ D \coloneqq \{v_i \mid M_1(v_i) = 0, M_2(v_i) = 0\} \end{cases} \tag{1}$$

Almost all common similarity measures (Sokal measure family, Sørensen-Dice, correlation etc.) can be defined with a,b,c,d. If one of the binary categorical variable can be considered as the truth, let's say M_2, therefore a becomes the number of *True Positives*, b of *False Positives*, c of *False Negatives* and d of *True Negatives*. We also trivially have the *Sensitivity*: $a/\left(a+c\right)$, *Specificity*: $d/\left(d+b\right)$, and the *Positive Predicted Value* (PPV): $a/\left(a+b\right)$. In fMRI, the v_i are the voxels and the variables M_1, M_2 are the functional maps to be compared (binary here, but the definition can easily be extended to probability maps).

3.2.1 Jaccard's index

When comparing two spatially distributed data, the most obvious measure is the Jaccard's index: the ratio between the size of their intersection and their union. It is defined by $J = a \;/\; (a+b+c)$ in our notation system. It provides intuitive and visual information about the overlap between one tested correlation map and one reference. It is also test-dependent: changing the risk or the multiple comparisons correction at the detection step will also change the shape and extent of the functional area, generally modifying Jaccard's index. This may be considered as a drawback but in fact, a statistical test is usually used at some point when investigating functional data.

3.2.2 Receiver operating characteristic analysis

In this section, we assume that the binary categorical variables are parameterized by at least one parameter. For example, in our case, it could be the risk for the statistical test of correlation α or a threshold on correlation r. Let r be our parameter, a_r, b_r, c_r, and d_r the previously defined cardinals in (1) now parametrized by r, and let define a set $\left\{\left(x\left(r\right), y\left(r\right)\right), r \in [-1, 1]\right\} \subset [0, 1]^2$ by:

$$\begin{cases} x(r) = 1 - \dfrac{d_r}{d_r + b_r} \\ y(r) = \dfrac{a_r}{a_r + c_r} \end{cases} \tag{2}$$

The implicitly defined function $f : x \mapsto y$ is called the *Receiver operating characteristic curve* (ROC-curve) and its integral $\int_0^1 f(x)dx$ is simply called the *Area Under Curve* (AUC). In the case where M_2 is considered to be the truth, f is just informally $f : 1 - Specificity \mapsto Sensitivity$. The AUC is not test-dependent as it covers all possible values of the threshold parameter (i.e. risk/correlation). It illustrates how a functional map *can* be close to the reference by considering *all* values of the considered parameter, while the Jaccard's index reflects how it *is* close to the reference by considering *one* value of the given parameter. Hence AUC is a better way to assess the trend of interest from a *theoretical* point of view. However, it is further away from the *practical* proximity of the Jaccard's index modeling offers, so we will eventually consider both scores.

3.3 Modeling trend with respect to the duration

Both Jaccard's index and AUC are computed for each subject, each seed, each duration and each functional network reference from MSDL. The next step is to model the trend of these two scores evolution according to the acquisition duration for all subjects and for each combination between one seed and one reference. Assuming rs-ASL sequence lasts long enough to cover all usage, extrapolation for a duration longer than 24 min 30 s seems superfluous. There is no theoretical model, even in BOLD, on the dependence between acquisition duration and quality of functional networks detection: we are not interested in an explicit formula. Moreover, even processed independently, neighboring within-subject time-points have a strong dependency as they come from the same acquisition. Under these conditions, a local non-parametric regression is very well-suited. We chose to use the Loess method. Loess can be understood as a local polynomial regression on a subset of the whole dataset, defined by a weighted K-nearest neighbors algorithm. For a more comprehensive description, see (29). We used second degree polynomial functions with a 0.8 span.

4 RESULTS

4.1 Effect of the acquisition duration for the Default Mode Network

In this section, we present an in-depth analysis of the DMN. In the set of 20 seeds we used, many should not be inspected when used in combination with MSDL DMN. The main reason is that most of the combinations has no objective basis for detecting the DMN. Otherwise, the seed may have failed to detect precisely the networks it was meant to detect, which is expected with very short acquisition duration. A good way to get an idea of the quality of the overlap between the functional maps associated with a seed and a reference for all durations is to check the boxplots of the Jaccard's index as in Figure 3. Boxplots give an overview of the results for rs-ASL: for the DMN reference, Jaccard's indices have higher values for the seeds placed in order to detect it. Prefrontal and posterior seeds seem to work well while lateral DMN seeds provide lower scores but still higher than any other seeds. Figure 4 shows the evolution of the estimated DMN with the prefrontal seed and corresponding scores for one subject. The depiction made by the scores of the overlap between the estimation of the DMN and the MSDL reference match with the four stages identified in Figure 2. Figure 5 shows the Jaccard's index, AUC, Sensitivity and Predicted Positive Value (PPV), for each subject and at each acquisition duration. Loess on Jaccard's index, as well as on AUC, models quite well what can be observed by looking directly at the functional map. Jaccard's index seems to stabilize after 12-13 min and AUC at an earlier acquisition duration around 9-10 min. We could have expected sensitivity and PPV to follow the same trend. Actually, sensitivity just grows over time, but more slowly for longer durations. Interestingly, PPV reaches a peak in the second stage mentioned above. The seven subjects show different level of response but good correlations (except for the subject 2

with AUC), i.e. the trend is the same among subjects, rather than an average effect induced by the Loess. Moreover results observed for the DMN, can be generalized for almost every combination of seeds and references as we will see.

4.2 Effect of the acquisition duration for all functional networks

Visual inspection of the acquisition data and of the estimated functional networks estimation is always a good practice (30) However, with more than 6000 functional maps generated (20 seeds, 7 subjects, 46 acquisition durations), a visual checking of all the maps is not practicable. As seen for DMN, many combinations between seeds and reference should not be investigated since they are not functionnally meaningful and will yield to very low overlapping scores (e.g. prefrontal seed with visual cortex). For Jaccard's index, we selected combinations for which at least 50% of observations have $J \geqslant 0.1$. For AUC, the median is also considered, with a threshold of 0.7. These thresholds on the median values may seem rather low, but let us remember that all the acquisition durations are taken into account, even the shortest ones. Figure 6 shows the median values for all the combinations between seeds and references. The two thresholds lead to an almost identical choice for the selection of combinations. All seeds have their best scores with the expected reference, and each of the six functional networks are considered to be sufficiently well detected with SBA for Jaccard's index in accordance with our selection rules. The AUC suggests as good enough one more seed for cerebellum but consider that salience is not detected well enough with our set of seeds.

Figure 7 shows the range of durations where scores are not significantly different from their maximum values (5% risk) for each selected reference/seed combination. Colors on heatmap are scaled between minimum and maximum values of the corresponding score and matches with the stages already described for DMN in the previous section. Indeed, for every combination between seeds and references, both scores rapidly increase, and start to stabilize after a certain duration. However, for both measures, the 95% confidence interval around the maximum suggests a later start in the stabilization than suggested directly by the Loess curve values. While some combinations scores look already stabilized at 12 min, almost all of them are close to their maximum value at 16 min. Figure 8 shows a collection of functional areas obtained at a duration of 14 min. While language seed struggles to detect spatial components far from the seeds, all the other ones provide good detection of expected functional networks. The two bottom rows show the same subjects and the same reference with different seeds.

5 DISCUSSION

5.1 On methods

In order to estimate functional networks, the two most common methods are SBA and Independent Component Analysis (ICA). We did not work with ICA because the association between independent components and functional areas of the brain is intrinsically tedious (31) (32), especially when it comes to comparison between subjects. Moreover, in order to investigate the relationship between quality and duration for all subjects, we must estimate the functional areas in the same way for each subject. Indeed, keeping the same seeds and the same test for SBA is trivial, while keeping the same number of independent components is equivocal, since it should be decided by a goodness of fit criterion.

We chose to report the positive predicted value rather than specificity for two main reasons. On the one hand, true negatives can have multiple definitions in fMRI, since it depends on the voxels considered: the whole volume, only the brain or any smaller ROI like grey matter. Although it is logical to consider

only brain voxels for functional activity, this implies an extremely high number of true negatives, since the volume of a functional network is ten to a hundred times smaller than the one of the whole brain. Therefore, the specificity reaches values too high to provide relevant information on similarity between functional areas. On the other hand, like specificity, PPV plays a similar role with respect to sensitivity: specificity gives a complementary information to sensitivity in the totality of voxels whereas PPV gives a complementary information in the union of the reference and the estimated functional area.

5.2 On results

Our two objectives were to confirm the feasibility of resting state ASL and to evaluate the influence of the acquisition duration on the estimation of functional areas. Figure 4 and Figure 8 with corresponding scores in Figure 6 and in Figure 7 confirm that, even with the basic preprocessing and straightforward methodology we used, ASL is fully viable as a resting-state method. Regarding the impact of acquisition duration, the most important result is the stabilization of the functional areas representation after a certain duration for both measures, Jaccard's index and AUC, with a strong inter-subjects correlation (i.e. not a mean-effect induced by the Loess modeling). Since the acquisition should have the shortest duration possible for clinical implementation, the recommended duration eventually corresponds to the start of the stabilization stage. Strict definitions of the stabilization stage lead to longer duration since they would rely heavily on the Loess maximum by considering as stable just a narrow interval around of the maximum. However, since after 12 min to 14 min the score variations are low, a slight change in preprocessing or in the population could also lead to unstable maximum, without changing the trend. Relaxed definitions would keep optimal duration stability, but they may consider a functional area as good enough when an human investigator would not. Actually, early stages of acquisition are associated with poor representation of functional areas disconnected from the seed. Based on our different results, 14 min seems to be an interesting compromise.

Note that the DMN, the sensori-motor cortex, and the cerebellum have an almost consensual spatial definition among the authors, unlike language, visual and salience, which show a greater spatial variability (see for example http://neurosynth.org/). As we provide an evaluation only with one set of references (from the MSDL), one could have expected this to be a limitation of our work. However the spatial variability of the areas of interest in atlases is low enough to change only the scores but not the trend observed in this paper. Preprocessing influence should also be considered as positive: since we use typical and basic preprocessing, more advanced techniques should provide the same or an earlier stabilization, still keeping our suggestion as a sufficient duration.

The same is true for ASL readout approach. Using a 3D readout is probably an improvement in our sequence, as it tends to outperform 2D EPI, but not every investigator has access to 3D sequence (13)[1]. Not to mention the resting-state and readout approach, ASL is very sensitive to changes in its parameters. Since we are studying the influence of acquisition duration for a given set of parameters, the optimal duration of 14 min could be strongly influenced by the sequence parameters. Although the influence of each of them is to be kept in mind, most of them should not disturb the investigators, as most of them have a specific bibliography that goes well beyond the issue of the optimal acquisition duration. However, two of them may have a deep impact on our results: post-labeling delay and repetition time (TR). As mentioned in section 2.2, we already have some clues on how the PLD can influence functional networks representation. The critical parameter in our opinion is repetition time. It defines the sample frequency of the resting-state

[1] It is anticipated that single-shot 3D readout may be the preferred option in the future, but these methods are not yet sufficiently well tested to recommend for general use at this time. Multislice singleshot 2D echo-planar imaging (EPI) or spiral readout should be considered a viable alternative to segmented 3D sequences, because they are available on all systems and are insensitive to image artifacts from motion.

signal and turning our 14 min suggestion into a 240 volumes since we only work numerically on the signal. Its variation may shift the stabilization step toward a higher/lower number of volumes and hence a longest/shortest duration, without changing the stabilization of the functional networks representation after a certain number of volumes (i.e. same signal but different sampling frequency). Moreover in rs-ASL, TR values are typically between 3 s and 5 s, which is too wide to assume the locally linear dependence between TR and optimal duration. As a preliminary work on optimal duration in rs-ASL, we focus more on the modeling rather than investigating the influence of the TR. However, a specific study on the relationship between repetition time, volume number and quality of acquisition would be, in our opinion, highly beneficial to better define the optimal duration and also would be useful when an investigator sets up a sequence.

Last, we work on a homogeneous sample of subjects. While it greatly limits the influence of variables related to the population description and not included in our modeling, it also narrows the population represented by our sample of subjects. Hence, a natural perspective is to include new subjects in order to extend the population represented and checks if the influence of variables like gender, age, laterality could be excluded from the population variability. It should be noted that geriatric, pediatric and pathologic populations should be treated separately rather than included. Indeed, these populations can show extreme differences in average (or local) perfusion, which possibly hinders the functional networks estimation, and hence, when the stabilization starts.

6 CONCLUSION

We model and process data in order to get results as close as an investigator would do. All the considered functional areas were well detected by rs-ASL. Our results show a quality stabilization after a certain volume number/duration for both scores in all but one combination between seeds and references: very long sequences should not hence be considered. The main objective was to answer ”How long is enough?”. While we can suggest, for our set of sequence parameters, the optimal volume number of 240 / optimal duration of 14 min, any methods that improves the detection of functional networks are likely to provide an earlier stabilization start, i.e. optimal volume number/duration. Since we use a basic and typical sequence, preprocessing and estimation, 240 volumes / 14 min even if not optimal should be enough for most rs-ASL usage. Last, the exploration of the impact of the TR and PLD on the optimal acquisition duration was beyond the scope of this article but would be highly beneficial for sequence implementation, since we forecast they are the two parameters that may shift the stabilization start toward higher number of volumes.

CONFLICT OF INTEREST STATEMENT

The authors declare that the research was conducted in the absence of any commercial or financial relationships that could be construed as a potential conflict of interest.

AUTHOR CONTRIBUTIONS

C.V. acquired the data with the help of the Neurinfo MRI research facility. C.V. designed research, performed research, analyzed data and wrote the paper. P.M, I.C, C.B. supervized all steps and corrected the paper.

ACKNOWLEDGMENTS AND FUNDINGS

MRI data acquisition was supported by the Neurinfo MRI research facility from the University of Rennes I. Neurinfo is granted by the the European Union (FEDER), the French State, the Brittany Council, Rennes Metropole, Inria, Inserm and the University Hospital of Rennes. This manuscript has been released as a pre-print at: `https://www.hal.inserm.fr/inserm-02129799v1`

DATA AVAILABILITY STATEMENT

In accordance with the consent form signed by the subjects, authors are not allowed to share MRI acquisitions. However, requests to see the raw data can be sent to the corresponding author. For the preprocessing steps we used Matlab CONN toolbox (www.nitrc.org/projects/conn, RRID:SCR_009550) (25). The rest of the code used for evaluation scores and Loess is available upon request from the corresponding author.

REFERENCES

1 .Biswal B, Yetkin Z, Haughton V, Hyde J. Functional connectivity in the motor cortex of resting human brain using echo-planar MRI. *Magnetic resonance in medicine : official journal of the Society of Magnetic Resonance in Medicine / Society of Magnetic Resonance in Medicine* **34** (1995) 537–41. doi:10.1002/mrm.1910340409.

2 .Van den Heuvel M, Hulshoff Pol H. Exploring the brain network: A review on resting-state fMRI functional connectivity. *European Neuropsychopharmacology* **20** (2010) 519–534. doi:10.1016/j.euroneuro.2010.03.008.

3 .Gao L, Wu T. The study of brain functional connectivity in Parkinson's disease. *Translational Neurodegeneration* **5** (2016) 1–7. doi:10.1186/s40035-016-0066-0.

4 .Agosta F, Pievani M, Geroldi C, Copetti M, Frisoni GB, Filippi M. Resting state fMRI in Alzheimer's disease: Beyond the default mode network. *Neurobiology of Aging* **33** (2012) 1564–1578. doi:10.1016/j.neurobiolaging.2011.06.007.

5 .Craddock C, Holtzheimer P, Hu X, Mayberg H. Disease state prediction from resting state functional connectivity. *Magnetic Resonance in Medicine* **62** (2009) 1619–1628. doi:10.1002/mrm.22159.

6 .Lynall ME, Bassett D, Kerwin R, McKenna PJ, Kitzbichler M, Muller U, et al. Functional Connectivity and Brain Networks in Schizophrenia. *Journal of Neuroscience* **30** (2010) 9477–9487. doi:10.1523/JNEUROSCI.0333-10.2010.

7 .Buxton R, Frank L, Wong E, Siewert B, Warach S, Edelman R. A general kinetic model for quantitative perfusion imaging with arterial spin labeling. *Mag. Res. Med.* **40** (1998) 383–396.

8 .Borogovac A, Asllani I. Arterial spin labeling (ASL) fMRI: Advantages, theoretical constrains and experimental challenges in neurosciences. *International Journal of Biomedical Imaging* **2012** (2012). doi:10.1155/2012/818456.

9 .Wang D, Alger J, Qiao J, Hao Q, Hou S, Fiaz R, et al. The value of arterial spin-labeled perfusion imaging in acute ischemic stroke: Comparison with dynamic susceptibility contrast-enhanced MRI. *Stroke* **43** (2012) 1018–1024. doi:10.1161/STROKEAHA.111.631929.

10 .Boissoneault J, Letzen J, Lai S, O'Shea A, Craggs J, Robinson M, et al. Abnormal resting state functional connectivity in patients with chronic fatigue syndrome: An arterial spin-labeling fMRI study. *Magnetic Resonance Imaging* **34** (2016) 603–608. doi:10.1016/j.mri.2015.12.008.

11 .Grade M, Hernandez Tamames JA, Pizzini F, Achten E, Golay X, Smits M. A neuroradiologist's guide to arterial spin labeling MRI in clinical practice. *Neuroradiology* **57** (2015) 1181–1202. doi:10.1007/s00234-015-1571-z.

12 .Mutsaerts H, Nordhøy W, Pizzini F, van Osch M, Zelaya F, Hendrikse J, et al. Multi-vendor reliability of arterial spin labeling perfusion MRI using a near-identical sequence: Implications for multi-center studies. *NeuroImage* **113** (2015) 143–152. doi:10.1016/j.neuroimage.2015.03.043.

13 .Alsop D, Detre J, Golay X, Günther M, Hendrikse J, Hernandez-Garcia L, et al. Recommended implementation of arterial spin-labeled Perfusion mri for clinical applications: A consensus of the ISMRM Perfusion Study group and the European consortium for ASL in dementia. *Magnetic Resonance in Medicine* **73** (2015) 102–116. doi:10.1002/mrm.25197.

14 .Alsop D, Dai W, Grossman M, Detre J. Arterial Spin Labeling Blood Flow MRI: Its Role in the Early Characterization of Alzheimer's Disease. *Journal of Alzheimer's Disease* **20** (2010) 871–880. doi:10.3233/JAD-2010-091699.

15 .Wolk D, Detre J. Arterial spin labeling MRI. *Current Opinion in Neurology* **25** (2012) 421–428. doi:10.1097/WCO.0b013e328354ff0a.

16 .Zhang N, Gordon M, Goldberg T. Cerebral blood flow measured by arterial spin labeling MRI at resting state in normal aging and Alzheimer's disease. *Neuroscience & Biobehavioral Reviews* **72** (2016) 168–175. doi:10.1016/j.neubiorev.2016.11.023.

17 .Van Dijk KRA, Hedden T, Venkataraman A, Evans KC, Lazar SW, Buckner RL. Intrinsic Functional Connectivity As a Tool For Human Connectomics: Theory, Properties, and Optimization. *Journal of Neurophysiology* **103** (2010) 297–321. doi:10.1152/jn.00783.2009.

18 .Bouix S, Swago S, West JD, Pasternak O, Breier A, Shenton ME. "Evaluating acquisition time of rfmri in the human connectome project for early psychosis. How much is enough?". *Lecture Notes in Computer Science (including subseries Lecture Notes in Artificial Intelligence and Lecture Notes in Bioinformatics)* (2017), vol. 10511 LNCS, 108–115. doi:10.1007/978-3-319-67159-8_13.

19 .Birn R, Molloy E, Patriat R, Parker T, Meier T, Kirk G, et al. The effect of scan length on the reliability of resting-state fMRI connectivity estimates. *NeuroImage* (2013). doi:10.1016/j.neuroimage.2013.05.099.

20 .Anderson JS, Ferguson MA, Lopez-Larson M, Yurgelun-Todd D. Reproducibility of single-subject functional connectivity measurements. *American Journal of Neuroradiology* **32** (2011) 548–555. doi:10.3174/ajnr.A2330.

21 .Laumann TO, Gordon EM, Adeyemo B, Snyder AZ, Joo SJ, Chen MY, et al. Functional System and Areal Organization of a Highly Sampled Individual Human Brain. *Neuron* **87** (2015) 657–670. doi:10.1016/j.neuron.2015.06.037.

22 .Chen J, Jann K, Wang D. Characterizing Resting-State Brain Function Using Arterial Spin Labeling. *Brain Connectivity* **5** (2015) 527–542. doi:10.1089/brain.2015.0344.

23 .Liang X, Tournier J, Masterton R, Connelly A, Calamante F. A k-space sharing 3D GRASE pseudo-continuous ASL method for whole-brain resting-state functional connectivity. *International Journal of Imaging Systems and Technology* **22** (2012) 37–43. doi:10.1002/ima.22006.

24 .Liang X, Connelly A, Calamante F. Graph analysis of resting-state ASL perfusion MRI data: Nonlinear correlations among CBF and network metrics. *NeuroImage* **87** (2014) 265–275. doi:10.1016/j.neuroimage.2013.11.013.

25 .Whitfield-Gabrieli S, Nieto-Castanon A. Conn : A Functional Connectivity Toolbox for Correlated and Anticorrelated Brain Networks. *Brain Connectivity* **2** (2012) 125–141. doi:10.1089/brain.2012.0073.

26 .Zhou D, Thompson W, Siegle G. MATLAB toolbox for functional connectivity. *NeuroImage* **47** (2009) 1590–1607. doi:10.1016/j.neuroimage.2009.05.089.

382 **27** .Eklund A, Nichols T, Knutsson H. Cluster failure: Why fMRI inferences for spatial extent have inflated
383 false-positive rates. *Proceedings of the National Academy of Sciences* **113** (2016) E4929–E4929.
384 doi:10.1073/pnas.1612033113.
385 **28** .Varoquaux G, Gramfort A, Pedregosa F, Michel V, Thirion B. Multi-subject dictionary learning
386 to segment an atlas of brain spontaneous activity. *Lecture Notes in Computer Science (including*
387 *subseries Lecture Notes in Artificial Intelligence and Lecture Notes in Bioinformatics)* **6801 LNCS**
388 (2011) 562–573. doi:10.1007/978-3-642-22092-0_46.
389 **29** .Cleveland W, Devlin S. Locally Weighted Regression: An Approach to Regression Analysis by Local
390 Fitting. *Journal of the American Statistical Association* **83** (1988) 596. doi:10.2307/2289282.
391 **30** .Power J. A simple but useful way to assess fMRI scan qualities. *NeuroImage* **154** (2017) 150–158.
392 doi:10.1016/j.neuroimage.2016.08.009.
393 **31** .McKeown M, Hansen L, Sejnowski T. Independent component analysis of functional MRI: What is
394 signal and what is noise? *Current Opinion in Neurobiology* **13** (2003) 620–629. doi:10.1016/j.conb.
395 2003.09.012.
396 **32** .Cole D, Smith S, Beckmann C. Advances and pitfalls in the analysis and interpretation of resting-state
397 FMRI data. *Frontiers in systems neuroscience* **4** (2010) 8. doi:10.3389/fnsys.2010.00008.
398 **33** .Behzadi Y, Restom K, Liau J, Liu T. A component based noise correction method (CompCor) for BOLD
399 and perfusion based fMRI. *NeuroImage* **37** (2007) 90–101. doi:10.1016/j.neuroimage.2007.04.042.

FIGURES

APPENDIX - SEED LOCATION IN MNI152

Expected networks	Seed	Location in MNI152
DMN	Prefrontal	(1,55,-3)
DMN	Left	(-39,-77,33)
DMN	Right	(47,-67,29)
DMN	Posterior	(1,-61,38)
Motor	Left	(-55,-12,29)
Motor	Right	(56,-10,29)
Motor	Superior	(0,-31,67)
Visual	Primary	(2,-79,12)
Visual	Ventral	(0,-93,-4)
Visual	Dorsal Left	(-37,-79,10)
Visual	Dorsal Right	(38,-72,13)
Salience	Cingulate Anterior	(0,22,35)
Salience	Prefrontal Left	(-32,45,27)
Salience	Prefrontal Right	(32,46,27)
Language	Frontal Gyrus Left	(-51,26,2)
Language	Frontal Gyrus Right	(54,28,1)
Language	Temporal Gyrus Left	(-57,-47,15)
Language	Temporal Gyrus Right	(59,-42,13)
Cerebellum	Anterior	(0,-63,-30)
Cerebellum	Posterior	(0,-79,-32)

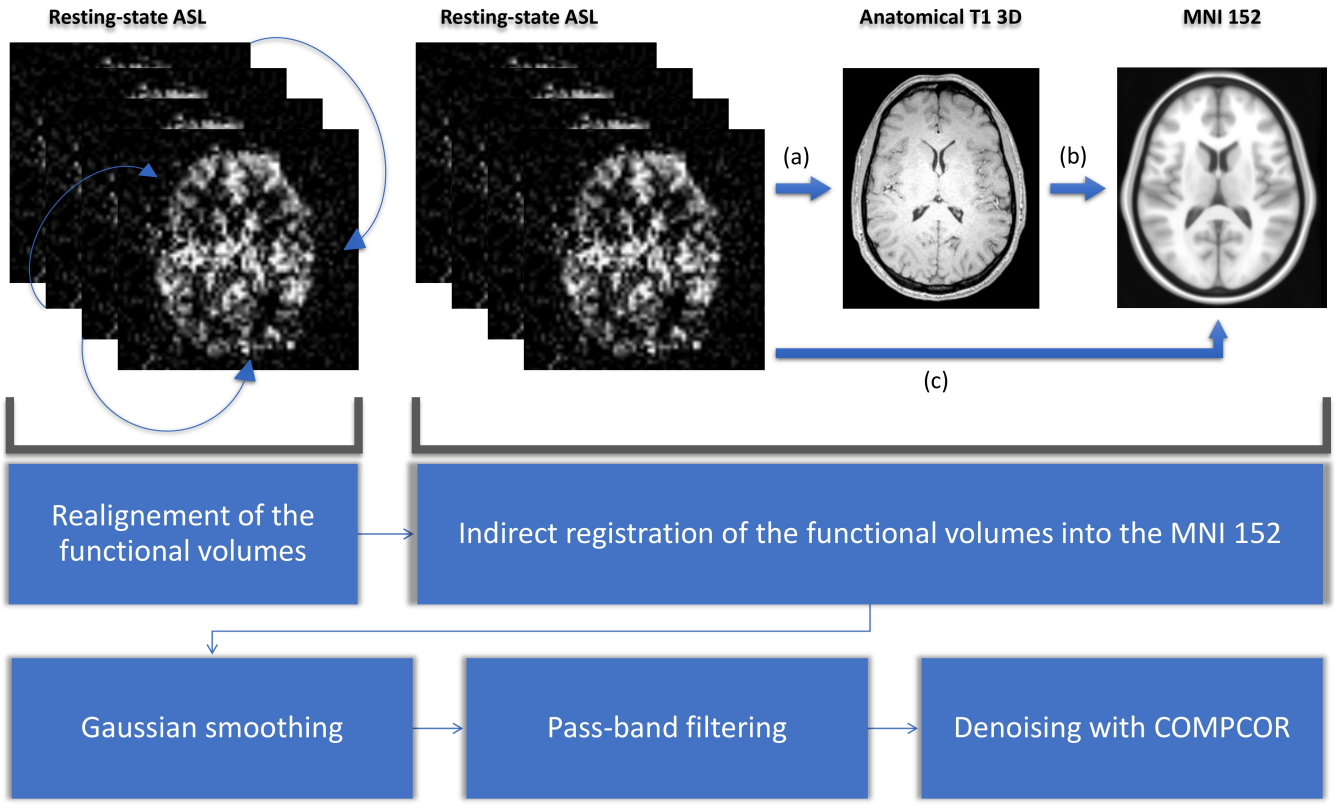

Figure 1. Preprocessing steps of the rs-ASL images. After a surround substraction of labels and controls, preprocessing starts with the realignment of the perfusion weighted-map. All the functional volumes are registered with the first one. Second step is the indirect normalization of the functional volumes. It starts with registration of the functional data on the anatomical 3D T1 (a). Then comes the registration of the anatomical image on the MNI 152 template (b). Finally, transformations of (a) and (b) are composed to register functional data on the MNI template (c). We then used Gaussian smoothing with typical 6 mm kernel and pass-band filtering with a range from 0.005 Hz to 0.1 Hz. Final denoising was made with COMPCOR (33).

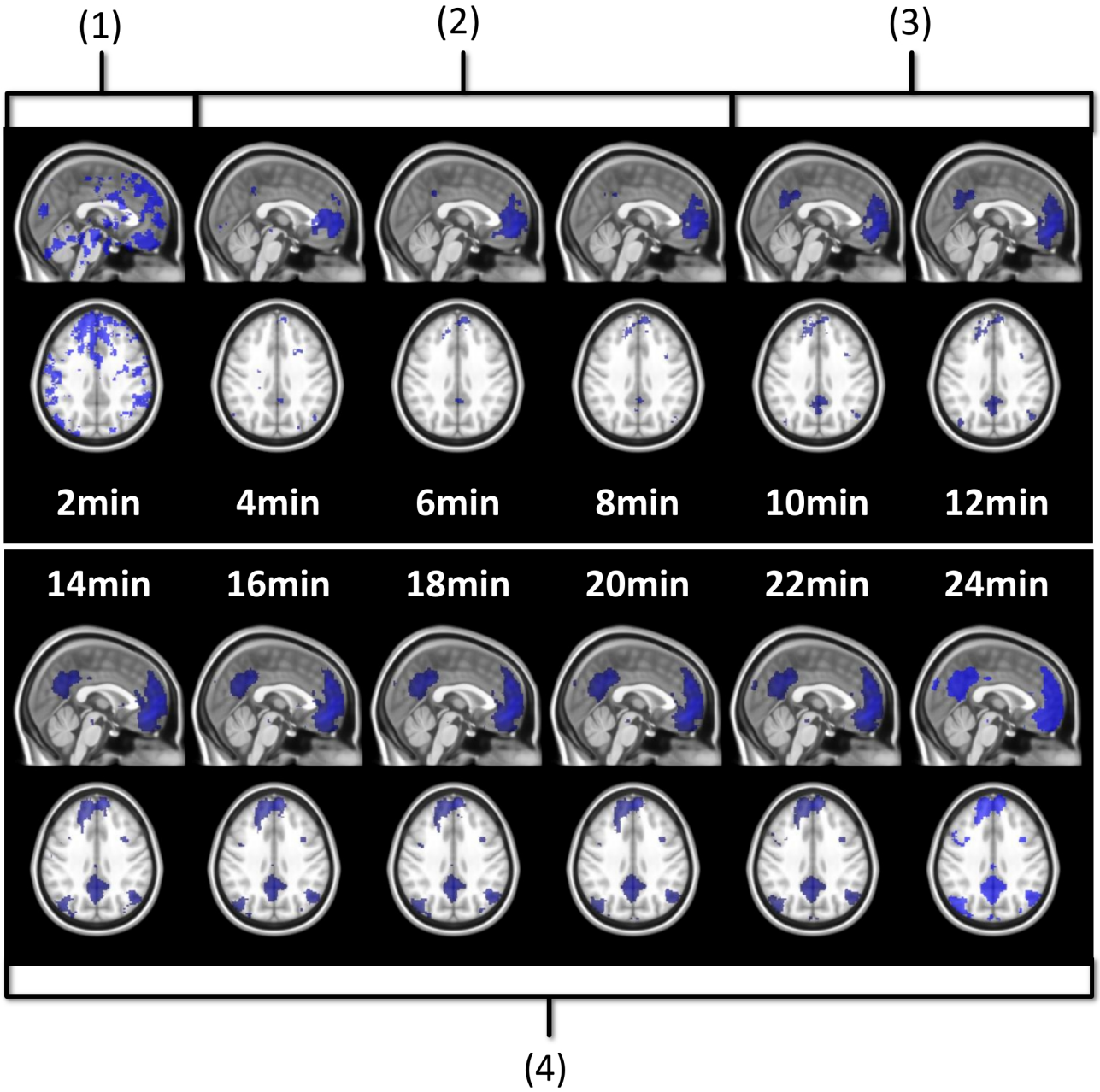

Figure 2. Seed-based estimation of the DMN with prefrontal seed at different acquisition durations. Four stages can be identified. At 2 min (1), the map shows only false positive noise detection. Between 4 min and 8 min (2), the false positive noise has disappeared while the frontal component of the DMN starts growing and the posterior starts being detected. Between 10 min and 12 min (3), the frontal component is well detected, the posterior grows and the lateral components are barely being detected. At 14 min and after (4), DMN detection is good and interestingly, stable.

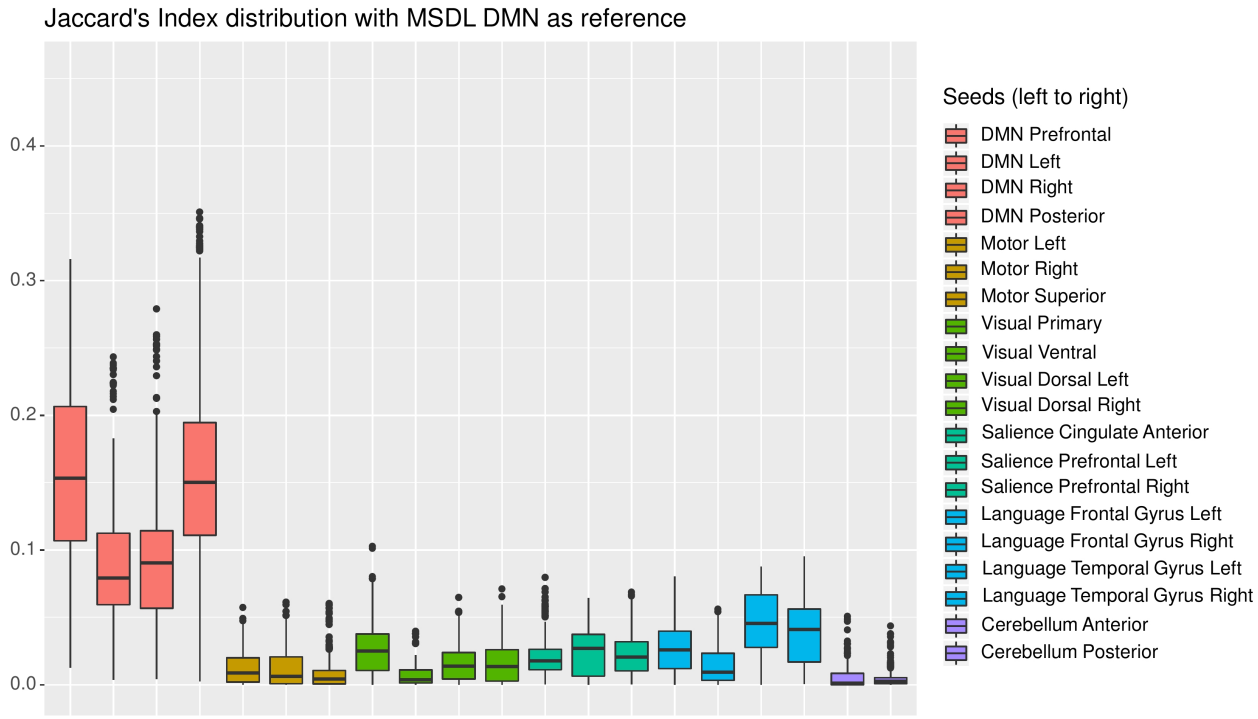

Figure 3. Each boxplot corresponds to one seed and shows the distribution of Jaccard's index between the estimated functional area corresponding to the considered seed on the one hand, and the MSDL DMN reference on the other hand, for all subjects and all durations. The seeds are grouped by color, each corresponding to one of the six functional areas considered. As expected, the seeds located in the expected DMN location (in pink) give the best results.

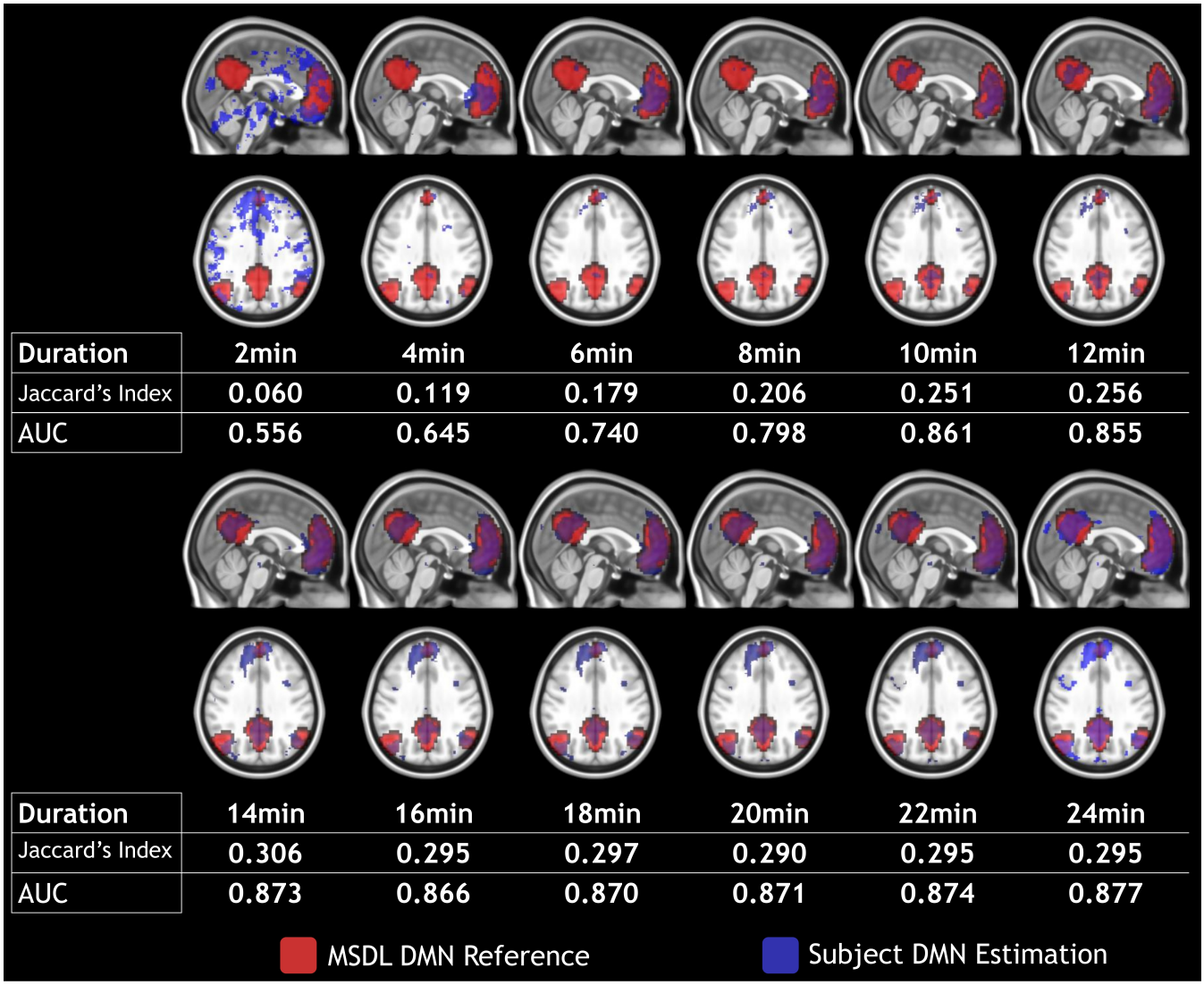

Figure 4. Subject 4 DMN detection (in blue) with prefrontal seed and MDSL DMN reference (in red) over a 2 min to 24 min duration with 2 min steps. Maps are shown in MNI152 space.

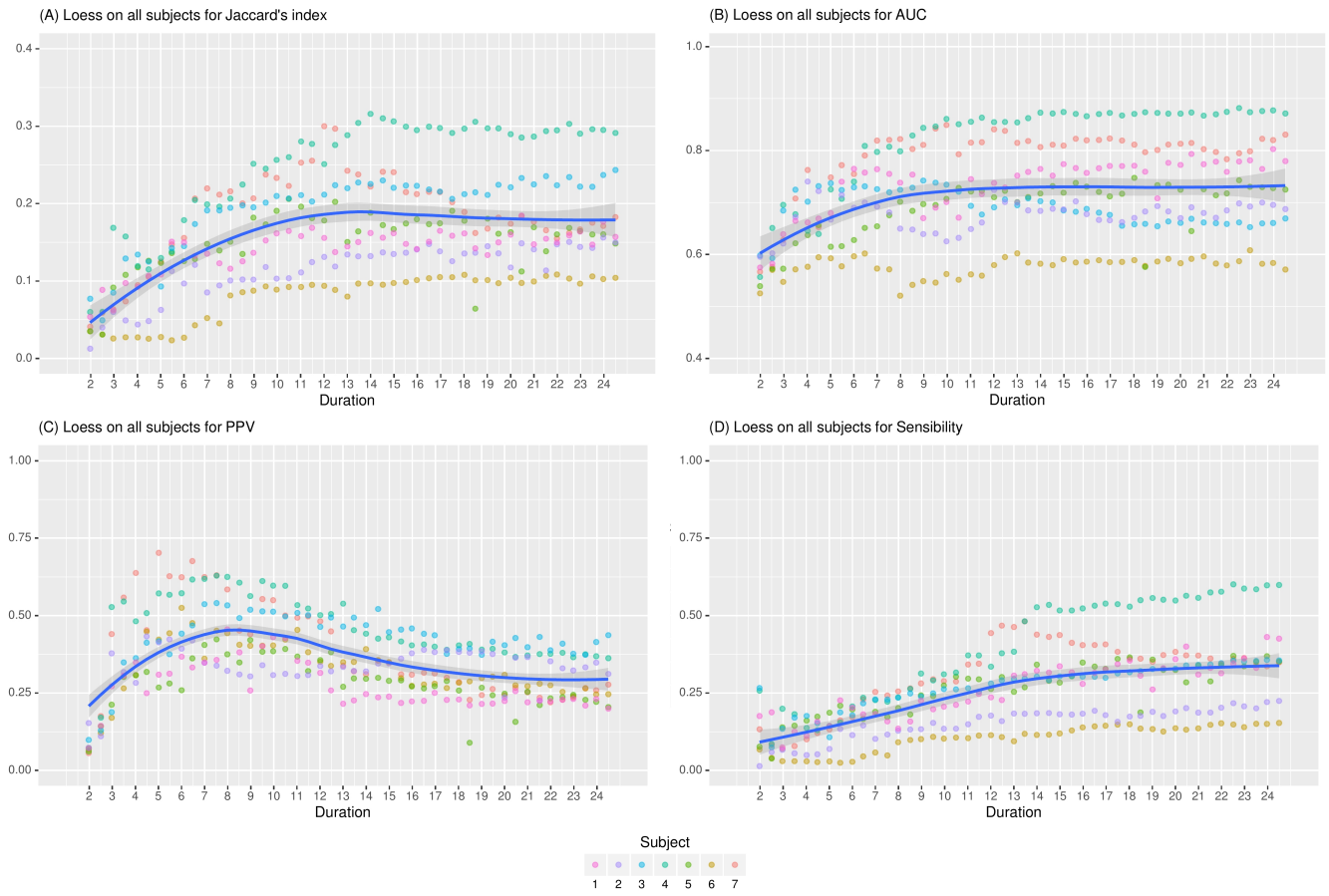

Figure 5. Jaccard's indices (A), AUC (B), Positive Predicted Value (C) and Sensibility (D) evolution with time with their associated Loess for the seed associated with prefrontal DMN. On all subjects, Jaccard's index increases with duration before 10-12 min, then stabilizes. The AUC shows the same trend with an earlier stabilization, around 9-10 min. PPV grows rapidly, reaches a peak at 8 min, then decreases slowly. Finally, Sensitivity increases with time, but more slowly for longer durations. Subjects show different level of response but good correlations.

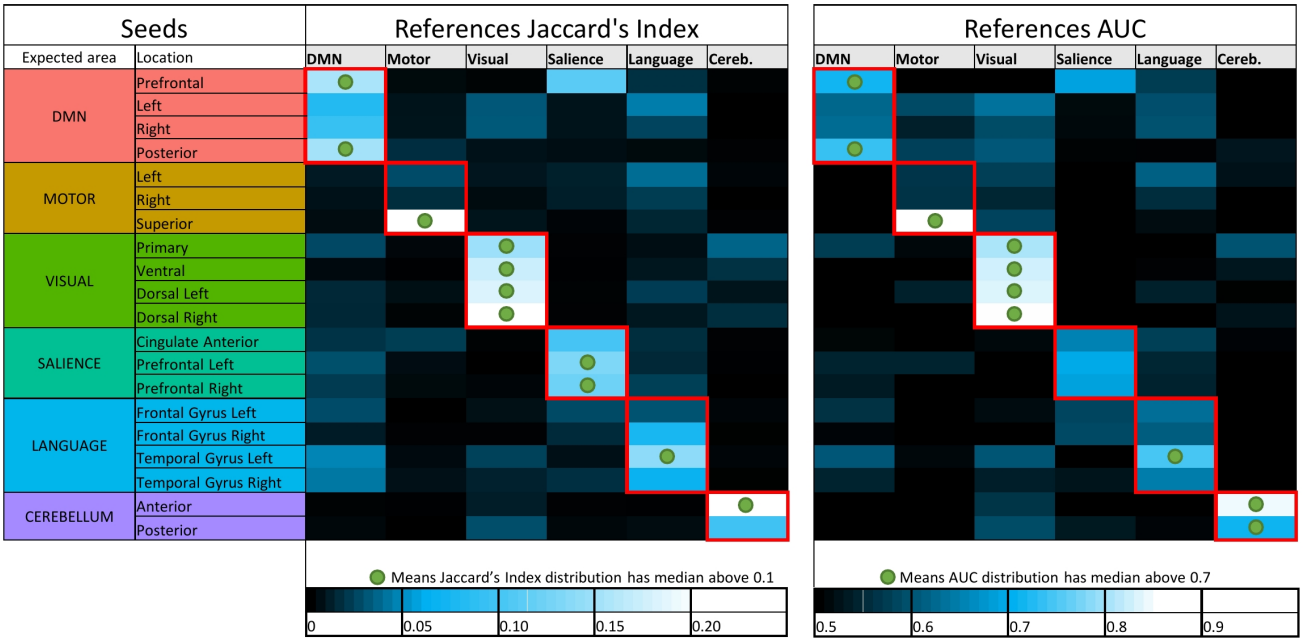

Figure 6. Median values of Jaccard's indices and AUC for all combinations of seeds/references. Green circles show where seeds/reference combinations are selected with respect to our thresholding rules (0.1 for the Jaccard median and 0.7 for the AUC median).

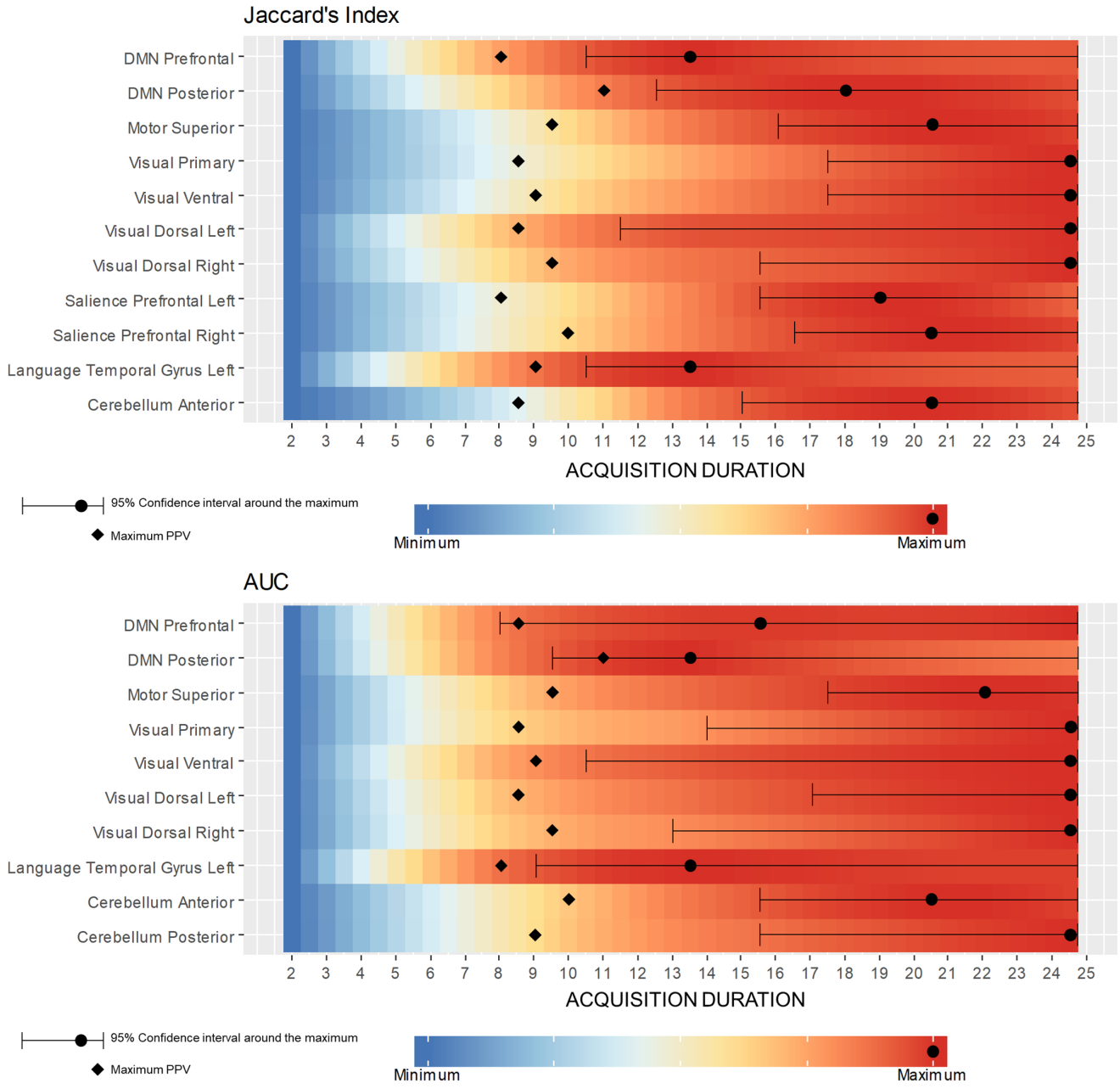

Figure 7. Color maps of Jaccard's Index and AUC Loess value with respect to the acquisition duration for all selected reference/seed combination. Every combination has a fast increasing score followed by a stabilization stage. The PPV peak shows on all combinations around 9 min and appears always just before score start stabilizing. Maximum and its 95% confidence interval may be unstable since score variations are often low after PPV peak.

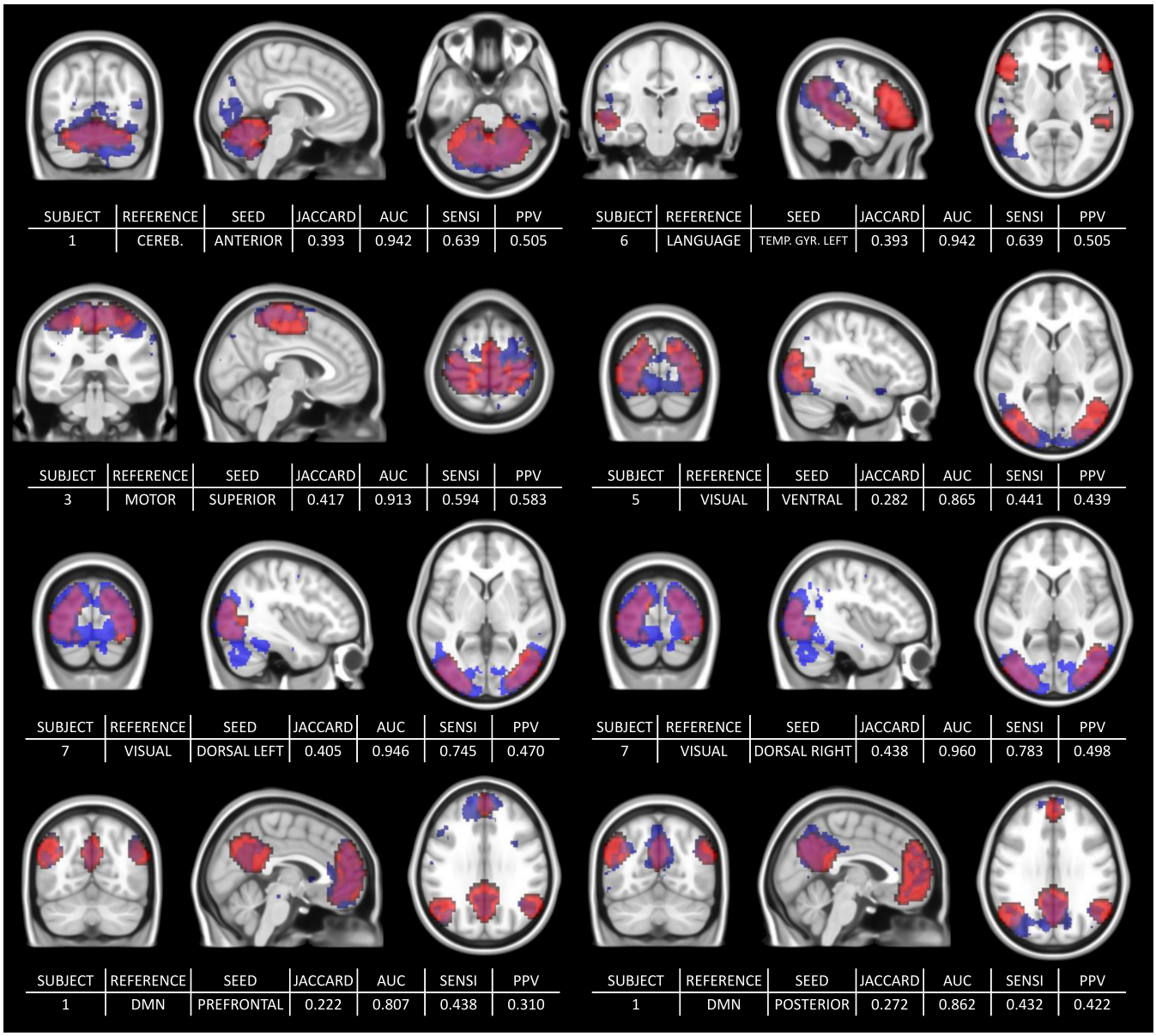

Figure 8. Collection of functional areas at 14 min with the corresponding scores: Jaccard's Index, Area Under the Curve, Sensitivity and PPV. The two bottom rows show the same subjects and the same reference but with different seeds. The third row shows the estimated (blue) and reference (red) visual network for the same subject (subject 7) but different seeds ("dorsal left" seed on the left and "dorsal right" seed on the right). Similarly, the bottom row shows the same subject (subject 1) with different seeds ("Prefrontal" and "Posterior").